Multimodality Imaging of Attenuated Plaque Using Grayscale and Virtual Histology Intravascular Ultrasound and Optical Coherent Tomography

Soo-Jin Kang[1], MD, PhD, Jung-Min Ahn[1], MD, Seungbong Han, PhD[2], Duk-Woo Park[1], MD, PhD, Seung-Whan Lee[1], MD, PhD, Young-Hak Kim[1], MD, PhD, Cheol Whan Lee[1], MD, PhD, Seong-Wook Park[1], MD, PhD, Gary S. Mintz[3], MD, Seung-Jung Park[1], MD, PhD

[1] Department of Cardiology, University of Ulsan College of Medicine
Asan Medical Center, Seoul, Korea
[2] Department of Biostatistics, University of Ulsan College of Medicine
Asan Medical Center, Seoul, Korea
[3] Cardiovascular Research Foundation,
New York, NY

Words count : 4891

Corresponding Author
Seung-Jung Park, MD., PhD.
Professor of Medicine
Asan Medical Center
388-1 Poongnap-dong, Songpa-gu
Seoul, South Korea, 138-736
Phone: 82-2-3010-4812
Fax: 82-2-475-6898
E-mail: sjpark@amc.seoul.kr

Abstract

Background Although attenuated plaque is a marker for plaque vulnerability, the quantification and its implication have not been known.

Methods Multimodality pre-procedural imaging using grayscale intravascular ultrasound (IVUS), virtual histology-IVUS (VH-IVUS) and optical coherence tomography (OCT) were performed in 115 coronary lesions with diameter stenosis (DS) >30% and plaque burden ≥50% and compared the diagnostic accuracies for detecting thin-cap fibroatheromas (TCFA).

Results A maximal arc of attenuation (40MHz IVUS) $\geq 29.0°$ was the cut-off for predicting VH-TCFA (sensitivity 74%, specificity 66%); and OCT-TCFA (sensitivity 89%, specificity 64%), while a maximal arc attenuation$\geq 29.0°$ (20MHz IVUS) showed a poor sensitivity for predicting TCFA. Compared to the lesions with an arc of attenuation<30° as a rough cut-off value, the lesions with a maximum arc of attenuation≥30° (40MHz) were associated with more severe (smaller angiographic minimum lumen diameter and greater DS, smaller IVUS-MLA and a larger plaque burden) and had more unstable lesion characteristics: (1) larger remodeling index and more plaque ruptures (grayscale IVUS); (2) greater %necrotic core and more VH-TCFAs (VH-IVUS); and (3) more lipid, macrophages, cholesterol crystals, and microchannels; thinner fibrous caps; and more OCT-TCFAs, OCT-detected plaque ruptures, and red and white thrombi (OCT). Among 58 patients treated with stent implantation, post-intervention peak CK-MB was higher in patients with the maximal attenuation$\geq 30°$ compared to those without (median 2.7 ng/ml [IQR 0.9-18.7 ng/ml] vs. median 0.9 ng/ml [IQR 0.7-2.1 ng/ml], p=0.012).

Conclusion Attenuated plaque with a maximal attenuation$\geq 30°$ vs. <30° (40MHz, but not 20MHz IVUS) were more likely to be associated with unstable lesion morphology that may contribute to the immediate post-stenting CK-MB elevation.

3

Key Words: vulnerable plaque, virtual histology, optical coherent tomography, attenuat

ed plaque

Introduction

Attenuated plaque (hypoechoic or mixed atheroma with ultrasound attenuation, but without calcification) detected by grayscale intravascular ultrasound (IVUS) is more common in patients with acute coronary syndrome than patients with stable angina and more common in patients with ST-elevation myocardial infarction than patients with non-ST-elevation myocardial infarction.[1-3] Virtual histology (VH)-IVUS and optical coherence tomographic (OCT) studies have shown that attenuated plaque is a marker for a large necrotic core and a thin cap fibroatheroma (TCFA).[4,5] Clinical studies have suggested that attenuated plaque is associated with a high-risk for no-reflow or post-procedural CK-MB elevation.[6,7] However, there are few studies quantifying the amount of grayscale attenuation that would predict a TCFA or comparing the differences between 40MHz vs. 20MHz IVUS since transducer frequency impacts on ultrasound penetration. Therefore, the aims of the current study were 1) to identify the extent of grayscale IVUS attenuation that predicts unstable lesion morphology assessed by VH-IVUS or OCT as well as post-procedure CK-MB release and 2) to compare the diagnostic accuracies of 40MHz vs 20MHz IVUS transducers.

Methods

Subjects. From November 2006 to June 2011, pre-procedural angiography, grayscale IVUS (using both 40MHz and 20MHz transducers), VH-IVUS, *and* OCT were performed in 161 patients. All had a lesion with a diameter stenosis (DS) >30% (visual estimation) within the proximal or mid segment of a native coronary artery with a plaque burden >50%. The current analysis excluded large vessel size >4.0mm (10 patients), left main or ostial lesions (before 2011, 9 patients), poor OCT image quality (9 patients), poor grayscale- or VH-IVUS image (4 patients), incomplete OCT evaluation in entire target segment (5 patients), inability of any of the three intravascular imaging devices to cross the lesion into the distal vessel due to a tight stenosis or severe vessel tortuousity (6 patients), sidebranch lesion (2 patients), and dissection during OCT procedure (1 patient). Finally, 115 patients with 115 coronary lesions (one lesion per patient - 63 left anterior descending, 15 left circumflex, and 37 right coronary artery lesions) were included. Informed consent for the imaging tests and coronary intervention was obtained before the procedure.

Angiographic analysis. Quantitative angiographic assessments were done using standard techniques with automated edge-detection algorithms (CASS-5, Pie-Medical, Netherlands) in the angiographic analysis center of the CardioVascular Research Foundation, Seoul, Korea. Angiographic diameter stenosis and lesion length were measured.

IVUS Imaging and Analysis. After intracoronary administration of 0.2mg nitroglycerin, grayscale IVUS imaging was performed using motorized pullback (0.5mm/s) of a rotating, 40-MHz transducer within a 3.2Fr imaging sheath and a commercial scanner (Boston Scientific/SCIMED, Minneapolis, MN, USA). Using computerized planimetry (EchoPlaque 3.0, Indec Systems, Mountain View, CA, USA), off-line quantitative IVUS analysis was performed in a core laboratory at the Asan Medical Center.[8]

Distal and proximal fiduciary branches and each ostium were used as landmarks for identical evaluation of target segment by the multimodality images. To ensure the same index site on grayscale- and VH-IVUS, and OCT images, the operator selected a distal fiduciary site as the beginning point for analysis.

External elastic membrane (EEM) and minimal lumen area (MLA) were measured. Plaque burden at the MLA site was calculated as EEM area minus lumen area divided by EEM area.[8] Remodeling index was defined as EEM area at the MLA site divided by the averaged reference EEM area. Plaque rupture was identified by the presence of a cavity that communicated with the lumen with an overlying residual fibrous cap fragment. Plaque attenuation was defined as ultrasonic attenuation of deeper arterial structures that began within the plaque despite the absence of calcium.[6,9,10] The length of the attenuation segment was measured. The maximal arc of attenuation was also measured in degrees by an electronic protractor, and included only the attenuated region without calcification (Figure 1 and 2); the interobserver variability of the arc of attenuation measurement was 5.2±2.0°. If there was more than one arc of attenuation in a given image slice, the arcs were added. All grayscale- and VH-IVUS determinations were based on the observations of two independent experienced reviewers (SJK and JMA) who were blinded to other data. Interobserver and intraobserver variability yielded good concordance for the diagnosis of attenuated plaque (κ=0.91 and κ=0. 95, respectively). Examples are shown in Figure 1 and Figure 2.

Grayscale IVUS was then repeated and VH-IVUS performed, again after intracoronary administration of 0.2mg nitroglycerin, using the 2.9Fr Eagle Eye IVUS catheter that incorporated a synthetic aperture array 20MHz transducer and a commercial scanner (Volcano Corp, Rancho Cordova, CA). The transducer was advanced distally, and an imaging run was performed back through the mid to proximal

coronary segments using the R-100 motorized pullback device (0.5mm/s). Then the attenuation length, the attenuation angle at the maximal attenuation site, and the attenuation angle at the cross-section corresponding to the site of maximal attenuation site on the 40MHz IVUS image were measured. VH-IVUS analysis was performed using pcVH software (Volcano Corporation, Rancho Cordova, CA). A region of interest was placed between the luminal and EEM borders; and tissue was coded as green (fibrotic), yellow-green (fibrofatty), white (dense calcium), and red (necrotic core).[11,12] Fibroatheromas were defined by the presence of >10% confluent necrotic core; a VH-TCFA had >30° of the necrotic core abutted the lumen (without overlying fibrous tissue) in ≥3 consecutive frames.[12,13] All VH-IVUS assessments were done within the length of the lesion, at the site of maximal attenuation seen with the 20 MHz transducer, and at the site of the maximal attenuation seen with the 40MHz transducer. Examples are shown in Figure 1.

OCT imaging and analysis. Before April 2011, OCT images were acquired using the proximal occlusive technique, the 0.019-in ImageWire, and a commercially available system (LightLab Imaging, Westford, MA).[14] The artery was cleared of blood by continuous flushing with iodixanol 370 (Visipaque, GE Health Care, Cork, Ireland) at a flow rate of 3.0 mL/s.[15] Since April 2011, OCT images were acquired using a non-occlusive technique with the C7XR™ system and DragonFly™ catheters (LightLab Imaging, Inc., Westford, MA, USA). Calcification was a signal-poor region with sharp borders. Lipid pool was a signal-poor region with diffuse borders.[16] Fibrous cap thickness was measured at its thinnest part twice and the average value was calculated. Lipid angle was measured at the frame of the largest arc of lipid within the lesion. OCT-TCFA had a fibrous cap thickness at the thinnest part ≤65μm and an angle of lipidic tissue ≥120°.[17-20] Plaque rupture was a break in the fibrous cap that connected the lumen with the underlying lipid pool.[17-20] Thrombi were masses protruding into the

lumen and discontinuous from the surface of the vessel wall. Red thrombi were high-backscattering protrusions with signal-free shadowing, and white thrombi were signal-rich, low backscattering projections into the lumen.[20,21] Macrophages were signal-rich, distinct, or confluent punctate regions that exceeded the intensity of background speckle noise, as described by the OCT Consensus Standards document.[20] Cholesterol crystals were thin, linear regions of high intensity.[20] A microchannel was a small vesicular or tubular structure with a diameter ≤200µm.[20] All reported OCT parameters required the agreement of two observers (SJK, and JMA). Examples are shown in Figure 1 and Figure 2.

Statistical analysis. All statistical analyses were performed using SPSS (version 10.0, SPSS Inc., Chicago, IL). Continuous variables are presented as median and inter-quartile range (IQR) and compared using non-parametric Mann-Whitney test. Categorical variables were expressed as counts and percentages and compared with χ^2 statistics or Fisher's exact test. Receiver-operating curve was used to assess the best cut-off values of maximal arc of attenuation predicting TCFA or plaque rupture with a maximal accuracy using MedCalc (MedCalc Software, Mariakerke, Belgium). The optimal cut-off was calculated using the Youden index. The sensitivity, specificity, positive predictive value (PPV), and negative predictive value (NPV) with their 95% confidence intervals (CI) were determined. A p value <0.05 was considered statistically significant.

Results

Baseline clinical and grayscale IVUS data in a total of 115 patients were summarized in Table 1. Overall, 35 (30%) patients presented with an acute coronary syndrome (24 unstable angina, 8 non-ST elevation myocardial infarction, and 3 ST elevation myocardial infarction). Lesions were located in proximal in 42% and mid segments in 58%. Angiographic diameter stenosis and lesion length were 51.0% (42.0 – 62.0%) and 16.6mm (12.7 – 23.7mm), respectively.

The maximal attenuation angle using the 40MHz IVUS transducer was 80.0° (IQR 18.0 – 130.0°), which was greater than that using the 20MHz transducer (0° [0– 45.0°], p<0.001). The length of the attenuated segment was 3.2mm (0.8–7.0mm) measured by 40MHz transducer. Figure 3 compared the maximal arc of attenuation on grayscale IVUS using the 40MHz transducer vs. the 20MHz transducer.

The maximal attenuation angle measured by 40MHz transducer showed significant, but weak correlations with HDL-cholesterol (r=-0.296, p=0.001), LDL-cholesterol (r=0.229, p=0.014), and peak pre-intervention CK-MB (r=0.265, p=0.006). Moreover, the maximal attenuation angle correlated with angiographic DS (r=0.305, p=0.001) and IVUS MLA (r=-0.265, p=0.004), plaque burden (r=0.558, p<0.001), averaged reference segment EEM area (r=0.305, p=0.001), and remodeling index (r=0.261, p=0.005).

VH-IVUS findings. The maximal attenuation angle using 40MHz IVUS transducer was associated with a greater %necrotic core (r=0.265, p=0.004) and %dense calcium (r=0.209, p=-0.025) and to a smaller %fibrous (r=-0.273, p=0.003) and %fibrofatty (r=-0.203, p=0.030) plaque.

Overall, 80 (70%) lesions had at least one VH-TCFA. On ROC analysis, a maximal attenuation angle ≥29.0° (40MHz IVUS) predicted the presence of a VH-TCFA with a sensitivity of 74% and a specificity of 66% (Figure 4A). Using the rough

cut-off value of a maximal arc of attenuation $\geq 30°$, the predictabilities of 40MHz vs. 20MHz grayscale IVUS for the presence of a VH-TCFA were also shown in Figure 4B.

OCT findings. Overall, an OCT-TCFA was seen in 57 (50%) lesions. The maximal attenuation angle assessed by 40MHz IVUS negatively correlated with the minimal fibrous cap thickness (r=-0.427, p<0.001). On ROC analysis, a maximal arc of attenuation assessed by 40MHz IVUS $\geq 29.4°$ predicted the presence of an OCT-TCFA (sensitivity 89%, specificity 64%, Figure 5A). In addition, 41 (36%) lesions also had an OCT-detected plaque rupture; a maximal attenuation angle assessed by 40MHz IVUS $\geq 65°$ predicted the presence of OCT-detected plaque rupture (sensitivity 83%, specificity 64%, Figure 5B). The predictabilities of 40MHz vs. 20MHz grayscale IVUS for the presence of an OCT-TCFA were shown in Figure 5C.

In lesions with a greater plaque burden (>70%), a maximal arc of attenuation assessed by 40MHz IVUS $\geq 29.4°$ predicted the presence of an OCT-TCFA with a sensitivity 96% and a specificity 43%, and the presence of plaque rupture with a sensitivity 92% and a specificity 31%.

IVUS, VH-IVUS, and OCT analysis according to the maximal arc of attenuation. Using the rough cut-off value of a maximal arc of attenuation $\geq 30°$ seen with the 40MHz IVUS transducer, grayscale IVUS, VH-IVUS, and OCT findings are shown in Tables 1-3. Compared to lesions with an arc of attenuation <30°, lesions with a maximum arc of attenuation ≥30° were more often seen in males, in patients with an acute coronary syndrome, and in patients with a low HDL-cholesterol and a high LDL-cholesterol. Furthermore, these lesions were more severe (smaller angiographic minimum lumen diameter and worst diameter stenosis and smaller IVUS-MLA with a larger plaque burden) and had more unstable lesion characteristics: (1) larger remodeling index and more plaque ruptures (grayscale IVUS); (2) greater %necrotic

core and more VH-TCFAs (VH-IVUS); and (3) more lipid, macrophages, cholesterol crystals, and microchannels; thinner fibrous caps; and more OCT-TCFAs, OCT-detected plaque ruptures, and red and white thrombi (OCT).

Among 35 patients who presented with an acute coronary syndrome, 26 (74%) had a maximal arc of attenuation ≥30°; the sensitivity and specificity of predicting an OCT-TCFA in these patients was 96% and 62%, respectively. Even in 80 patients who presented with stable angina, 45 lesions (56%) had a maximal arc of attenuation ≥ 30°; the sensitivity and specificity of predicting an OCT-TCFA in patients with stable angina was 83% and 64%, respectively.

Tissue characteristics at the maximal attenuation site in 71 lesions with a maximal arc of attenuation ≥30° by 40MHz IVUS are shown in Table 4.The agreement rate between VH-IVUS and OCT for identifying TCFA at this site was 66%.

In 80 patients with stable angina, 45 (56%) had lesions with attenuation ≥30° by 40MHz IVUS. Compared to the lesions with attenuation <30°, the lesions with attenuation ≥30° showed more frequent VH-TCFA (87% vs. 54%, p=0.001) and OCT-TCFA (64% vs. 17%, p<0.001), more plaque ruptures (53% vs. 11%, p<0.001), and thinner fibrous cap (60.0μm [50.0 – 90.0μm] vs. 120.0μm [80.0 – 170.0μm], p<0.001).

40MHz vs 20MHz IVUS. Compared to the 41 lesions with the maximal attenuation ≥ 30° by 40MHz IVUS, but <30° by 20MHz, the 30 lesions with a maximal attenuation ≥ 30° on both 40MHz and 20MHz IVUS showed similar frequency of OCT-TCFA (46% vs. 60%, p=0.255), VH-TCFA (51% vs. 40%, p=0.349), and OCT-detected plaque rupture (44% vs. 47%, p=0.817) at the corresponding attenuation site. On ROC analysis, any attenuation (the maximal attenuation >0°) using a 20MHz transducer predicted either a VH-TCFA or an OCT-TCFA; however, the AUCs were only 0.563 and 0.693, respectively, and the sensitivities and specificities were 29% and 80% (for predicting a

11

VH-TCFA) and 46% and 93% (for predicting an OCT-TCFA).

Immediate post-stenting outcome. Stenting was performed in 58 (50%) patients, and no patient developed no-reflow. While there was no significant difference in pre-procedural peak CK-MB (median 1.0 ng/ml [IQR 0.6-2.4 ng/ml] vs. median 0.8 ng/ml [IQR 0.4 -1.1 ng/ml], p=-0.074), post-stenting peak CK-MB was higher in 40 patients with a maximal arc of attenuation ≥30° (40MHz IVUS) compared 18 patients with a maximal arc of attenuation <30° (median 2.7 ng/ml [IQR 0.9-18.7 ng/ml] vs. median 0.9 ng/ml [IQR 0.7-2.1 ng/ml], p=0.012). Post-stenting peak CK-MB >5.0 ng/ml was more common in patients with a maximal arc of attenuation ≥30° (40MHz IVUS) than in patients with a maximal arc of attenuation <30° (43% vs. 6%, p=0.007).

Discussion

The major findings of this study of lesions with grayscale IVUS plaque attenuation are the following. (1) The extent of attenuation was related to patient age, gender, unstable clinical presentation, serum levels of HDL- and LDL-cholesterol, and stenosis severity and remodeling. (2) Because 92% of lesions had at least a minimum amount of attenuation, this study focused on defining significant and clinically important attenuation. As such, a maximal attenuation angle ≥30° using a 40MHz transducer predicted the presence of a VH-TCFA (sensitivity 74% and specificity 66%) and an OCT-TCFA (sensitivity 89% and specificity 64%) as well as post-stenting peak CK-MB elevation.

Attenuated plaque has been considered to be a surrogate of unstable lesion characteristics and a predictor of no-reflow or post-procedural CK-MB elevation.[4-7] By concomitant use of grayscale IVUS, VH-IVUS, and OCT, our current analysis provided head-to-head comparisons of the tissue characteristics of attenuated plaque. Similar to previous data,[4,5] the extent of plaque attenuation positively correlated with necrotic core and dense calcium and negatively correlated with fibrous cap thickness. However, this current study also suggested that a maximal attenuation angle ≥30° predicted both a VH-TCFA and an OCT-TCFA with modest correlation (AUC 0.684 and 0.776, respectively), and that a maximal attenuation angle ≥65° predicted an OCT-detected plaque rupture which is more sensitive than IVUS-detected plaque rupture.[22] In addition, attenuated plaques in the current study were frequently associated with the presence of other unstable OCT findings such as macrophage infiltration, cholesterol crystal, microchannels, and thrombi. In the subgroup with a greater plaque burden >70%, the specificity of a maximal arc of attenuation by 40MHz IVUS ≥30° for detecting OCT-TCFA and plaque rupture was only 43% and 31%, respectively. Thus, IVUS attenuation seemed to be not specific for the prediction of TCFA or rupture especially in

13

the setting of a large plaque burden.

Previous studies reported that the presence of microchannels was related to plaque vulnerability and subsequent disease progression.[23,24] In this study, the higher frequency of microchannels in the lesions with attenuation ≥30° vs. <30° (40MHz) also suggested the relationship between IVUS attenuation and the presence of unstable atherosclerotic plaque.

Lee et al. reported that an attenuated plaque reflected biological instability only in patients with acute coronary syndrome,[1] whereas other studies identified a significant number of attenuated plaques in stable lesions.[5,25] In this current study a maximal arc of attenuation ≥30° predicted OCT-TCFA in patients with acute coronary syndrome with a high sensitivity of 96%; however, this cut-point was also a predictor of an OCT-TCFA in patients with stable angina with a sensitivity of 83%.

In the current analysis a greater arc of attenuation was associated with CK-MB elevation immediate post-stenting, consistent with the previous observations.[5-7] Thus, as a marker of vulnerability, plaque attenuation may have an impact on risk stratification and be of prognostic value regarding immediate PCI outcomes.

Previous studies evaluated attenuated plaque using either 20MHz or 40MHz transducers, but not both. Wu et al. demonstrated that the frequency of attenuated plaque assessed by 20MHz transducer was 44% in patients with ST-elevation myocardial infarction and 56% in those with non-ST elevation myocardial infarction.[5]

Our current data suggested that the 20MHz transducer with its greater penetration and lower frame rate consistently underestimated the extent of attenuation compared to the 40MHz transducer. Among lesions with a maximal arc of attenuation ≥30° assessed by a 40MHz transducer, only 42% showed a maximal arc of attenuation ≥30° on the 20MHz IVUS image. Lesions with 40MHz-IVUS attenuation

≥30°, but without significant 20MHz-IVUS attenuation had high frequencies of OCT-TCFA (46%), VH-TCFA (51%), and OCT-detected plaque rupture (44%). A maximal arc of attenuation ≥30° using the 20MHz transducer had a poor sensitivity (31%) and NPV (33%) in predicting a VH-TCFA and, despite a high specificity of 91%, a low sensitivity (49%) and NPV (65%) for the predicting an OCT-TCFA.

Compared with PROSPECT trial evaluating non-culprit lesions[13], the frequency of TCFA was relatively higher in this study, which was explained by including more severe lesions with advanced atherosclerosis; angiographic stenosis >50% was seen in 51% (vs. 6% in PROSPECT) and plaque burden >70% was shown in 72% (vs. 9% in PROSPECT).

Previous studies have reported the rates of agreement between VH-IVUS and OCT in the detection of TCFA.[26-27] Sawada et al. suggested that VH-IVUS and OCT agreed in 67% of lesions. Similarly, our current data showed that the agreement rate between VH-IVUS and OCT in detecting a TCFA at the maximal attenuation site was 66%. There are several methodological limitations that may contribute to mismatched findings. OCT attenuation caused by large amounts of red thrombus obscured underlying plaque morphology that might have lead to an underestimation of the frequencies of TCFA and rupture. Conversely, OCT potentially overestimates the incidence of TCFA due to foamy macrophages on the luminal surface that can be misinterpreted as a TCFA.[28] Conversely, VH-IVUS assessment of a TCFA may be limited by low spatial and temporal resolution and artifacts. Moreover, the incidence of VH-TCFA and %necrotic core might be underestimated in lesions with mural thrombi that are classified as fibrotic or fibrofatty plaque and may separate the necrotic core from the lumen.

Limitations. First, the present study is not a study of the natural history of lesions with attenuated plaque. Without follow-up data, we could not demonstrate the impact of the

findings on the long-term clinical outcomes. Second, we included only lesions that were suitable for OCT evaluation. Third, signal attenuation caused by thrombi possibly obscured major structures behind thrombi and distorted OCT image may limit the accurate assessment of lumen and plaque morphology. Although the arc of lipid pool > 90–180° has been used as the criteria for detecting OCT-TCFA,[17-20] the arc angle threshold still remains unclear. Finally, future pathologic studies are necessary to validate the imaging findings.

Conclusion. This multimodality imaging study showed that a maximal arc of grayscale IVUS (40MHz) attenuation $\geq$30° vs. <30° were more likely to be associated with unstable lesion morphologies (both VH-TCFA and OCT-TFCA) that may contribute to immediate post-stenting CK-MB elevation. But, the accurate detection of TCFA may be limited by the poor specificity, especially when the lesions have a large plaque burden.

Sources of Funding

18

Disclosures

We have no conflicts to disclose.

References

1. Lee SY, Mintz GS, Kim SY, Hong YJ, Kim SW, Okabe T, Pichard AD, Satler LF, Kent KM, Suddath WO, Waksman R, Weissman NJ. Attenuated plaque detected by intravascular ultrasound: clinical, angiographic, and morphologic features and post-percutaneous coronary intervention complication in patients with acute coronary syndromes. J Am Coll Cardiol Intv 2009;2:65–72.

2. Xu K, Mintz GS, Kubo T, Wu X, Guo N, Yang J, Witzenbichler B, Guagliumi G, Brodie B, Dressler O, Cristea E, Parise H, Mehran R, Stone GW, Maehara A. Long-term follow-up of attenuated plaques in patients with acute myocardial infarction: an intravascular ultrasound substudy of the HORIZONS-AMI trial. Circ Cardiovasc Interv 2012;5:185-92.

3. Okura H, Taguchi H, Kubo T, Toda I, Yoshida K, Yoshiyama M. Atherosclerotic plaque with ultrasonic attenuation affects coronary reflow and infarct size in patients with acute coronary syndrome: an intravascular ultrasound study. Circ J 2007;71:648–53.

4. Amano H, Wagatsuma K, Yamazaki J, Ikeda T. Virtual histology intravascular ultrasound analysis of attenuated plaque and ulcerated plaque detected by gray scale intravascular ultrasound and the relation between the plaque composition and slow flow/no reflow phenomenon during percutaneous coronary intervention. J Interv Cardiol 2013;26:295-301.

5. Wu X, Maehara A, Mintz GS, Kubo T, Xu K, Choi SY, He Y, Guo N, Moses JW, Leon MB, De Bruyne B, Serruys PW, Stone GW. Virtual histology intravascular ultrasound analysis of non-culprit attenuated plaques detected by grayscale intravascular ultrasound in patients with acute coronary syndromes. Am J Cardiol 2010;105:48-53.

6. Wu X, Maehara A, Mintz GS, Kubo T, Xu K, Choi SY, He Y, Guo N, Moses JW, Leon MB, De Bruyne B, Serruys PW, Stone GW. The relationship between attenuated plaque identified by intravascular ultrasound and no-reflow after stenting in acute myocardial infarction: the HORIZONS-AMI (Harmonizing Outcomes With Revascularization and Stents in Acute Myocardial Infarction) trial. JACC Cardiovasc Interv 2011;4:495-502.

7. Lee T, Kakuta T, Yonetsu T, Takahashi K, Yamamoto G, Iesaka Y, Fujiwara H, Isobe M. CK-MB Assessment of echo-attenuated plaque by optical coherence tomography and its impact on post-procedural creatine kinase-myocardial band elevation in elective stent implantation. JACC Cardiovasc Interv 2011;4:483-91.

8. Mintz GS, Nissen SE, Anderson WD, Bailey SR, Erbel R, Fitzgerald PJ, Pinto FJ, Rosenfield K, Siegel RJ, Tuzcu EM, Yock PG. American College of Cardiology Clinical Expert Consensus Document on Standards for Acquisition, Measurement and Reporting of IntravascularUltrasound Studies (IVUS). A report of the American College of Cardiology Task Force on Clinical Expert Consensus Documents. J Am Coll Cardiol 2001;37:1478-92.

9. Pu J, Mintz GS, Biro B, Lee JB, Sum ST, Madden SP, Burke AP, Zhang P, Zhao Y, Goldstein JA, Stone GW, Virmani R, Muller JE, Maehara A. Insights into echo-attenuated plaques, echolucent plaques, and plaques with spotty ultrasonic calcification: novel findings from comparisons between intravascular ultrasound and pathological histology in 2294 human coronary artery segments. *J Am Coll Cardiol 2014* In press

10. Pu J, Mintz GS, Brilakis ES, Banerjee S, Abdel-Karim AR, Maini B, Biro S, Lee JB, Stone GW, Weisz G, Maehara A. In vivo characterization of coronary plaques: novel findings from comparing greyscale and virtual histology intravascular ultrasound and near-infrared spectroscopy. *Eur Heart J* 2012**;33**:372-383.

11. Nair A. Kuban BD, Tuzcu EM, Schoenhagen P, Nissen SE, Vince G. Coronary plaque classification with intravascular ultrasound radiofrequency data analysis. Circulation 2002;106:2200–6.

12. Rodriguez-Granillo GA, García-García HM, Mc Fadden EP, Valgimigli M, Aoki J, de Feyter P, Serruys PW. In vivo intravascular ultrasound-derived thin-cap fibroatheroma detection using ultrasound. J Am Coll Cardiol 2005;46:2038-42.

13. Stone GW, Maehara A, Lansky AJ, de Bruyne B, Cristea E, Mintz GS, Mehran R, McPherson J, Farhat N, Marso SP, Parise H, Templin B, White R, Zhang Z, Serruys PW; PROSPECT Investigators. A prospective natural-history study of coronary atherosclerosis. N Engl J Med 2011;364:226-35.

14. *Xie Y, Takano M, Murakami D, Yamamoto M, Okamatsu K, Inami S, Seimiya K, Ohba T, Seino Y, Mizuno K. Comparison of neointimal coverage by optical coherence tomography of a sirolimus-eluting stent versus a bare metal stent three months after implantation. Am J Cardiol 2008;102:27–31.*

15. Gonzalo N, Garcia-Garcia HM, Regar E, Barlis P, Wentzel J, Onuma Y, Ligthart J, Serruys PW. In vivo assessment of high-risk coronary plaques at bifurcations with combined intravascular ultrasound virtual histology and optical coherence tomography. J Am Coll Cardiol Img 2009;2:473-82.

16. Yabushita H, Bouma BE, Houser SL, Aretz HT, Jang IK, Schlendorf KH, Kauffman CR, Shishkov M, Kang DH, Halpern EF, Tearney GJ. Characterization of human atherosclerosis by optical coherence tomography. Circulation 2002;106:1640–5.

17. Prati F, Regar E, Mintz GS, Arbustini E, Di Mario C, Jang IK, Akasaka T, Costa M, Guagliumi G, Grube E, Ozaki Y, Pinto F, Serruys PW; Expert's OCT Review Document. Expert review document on methodology, terminology, and clinical applications of optical coherence tomography: physical principles, methodology of image acquisition, and clinical application for assessment of coronary arteries and

atherosclerosis. Eur Heart J 2010;31:401-15.

18. Jang IK, Tearney GJ, MacNeill, Takano M, Moselewski F, Iftima N, Shishkov M, Houser S, Aretz HT, Halpern EF, Bouma BE. In vivo characterization of coronary atherosclerotic plaque by use of optical coherence tomography. Circulation 2005;111:1551–5.

19. Miyamoto Y, Okura H, Kume T, Kawamoto T, Neishi Y, Hayashida A, Yamada R, Imai K, Saito K, Yoshida K. Plaque characteristics of thin-cap fibroatheroma evaluated by OCT and IVUS. JACC Cardiovasc Imaging. 2011;4:638-46.

20. Tearney GJ, Regar E, Akasaka T, Adriaenssens T, Barlis P, Bezerra HG, Bouma B, Bruining N, Cho JM, Chowdhary S, Costa MA, de Silva R, Dijkstra J, Di Mario C, Dudek D, Falk E, Feldman MD, Fitzgerald P, Garcia-Garcia HM, Gonzalo N, Granada JF, Guagliumi G, Holm NR, Honda Y, Ikeno F, Kawasaki M, Kochman J, Koltowski L, Kubo T, Kume T, Kyono H, Lam CC, Lamouche G, Lee DP, Leon MB, Maehara A, Manfrini O, Mintz GS, Mizuno K, Morel MA, Nadkarni S, Okura H, Otake H, Pietrasik A, Prati F, Räber L, Radu MD, Rieber J, Riga M, Rollins A, Rosenberg M, Sirbu V, Serruys PW, Shimada K, Shinke T, Shite J, Siegel E, Sonoda S, Suter M, Takarada S, Tanaka A, Terashima M, Thim T, Uemura S, Ughi GJ, van Beusekom HM, van der Steen AF, van Es GA, van Soest G, Virmani R, Waxman S, Weissman NJ, Weisz G; International Working Group for Intravascular Optical Coherence Tomography (IWG-IVOCT). Consensus standards for acquisition, measurement, and reporting of intravascular optical coherence tomography studies: a report from the International Working Group for Intravascular Optical Coherence Tomography Standardization and Validation. J Am Coll Cardiol 2012;59:1058-72.

21. Kume T, Akasaka T, Kawamoto T, Ogasawara Y,Watanabe N, Toyota E, Neishi Y, Sukmawan R, Sadahira Y, Yoshida K. Assessment of coronary arterial thrombus by Optical Coherence Tomography. Am J Cardiol 2006;97:1713–7.

22. Kubo T, Imanishi T, Takarada S, Kuroi A, Ueno S, Yamano T, Tanimoto T, Matsuo Y, Masho T, Kitabata H, Tsuda K, Tomobuchi Y, Akasaka T. Assessment of culprit lesion morphology in acute myocardial nfarction: ability of optical coherence tomography compared with intravascular ultrasound and coronary angioscopy. J Am Coll Cardiol 2007;50:933-9

23. Uemura S, Ishigami K, Soeda T, Okayama S, Sung JH, Nakagawa H, Somekawa S, Takeda Y, Kawata H, Horii M, Saito Y.Thin-cap fibroatheroma and microchannel findings in optical coherence tomography correlate with subsequent progression of coronary atheromatous plaques. Eur Heart J 2012;33:78-85.

24. Kitabata H, Tanaka A, Kubo T, Takarada S, Kashiwagi M, Tsujioka H, Ikejima H, Kuroi A, Kataiwa H, Ishibashi K, Komukai K, Tanimoto T, Ino Y, Hirata K, Nakamura N, Mizukoshi M, Imanishi T, Akasaka T. Relation of microchannel structure identified by optical coherence tomography to plaque vulnerability in patients with coronary artery disease. Am J Cardiol. 2010;105:1673-8.

25. Kimura S, Kakuta T, Yonetsu T, Suzuki A, Iesaka Y, Fujiwara H, Isobe M. Clinical significance of echo signal attenuation on intravascular ultrasound in patients with coronary artery disease. Circ Cardiovasc Interv 2009;2:444–54.

26. Kubo T, Nakamura N, Matsuo Y, Okumoto Y, Wu X, Choi SY, Komukai K, Tanimoto T, Ino Y, Kitabata H, Kimura K, Mizukoshi M, Imanishi T, Akagi H, Yamamoto T, Akasaka T. Virtual histology intravascular ultrasound compared with optical coherence tomography for identification of thin-cap fibroatheroma. Int Heart J 2011;52:175-9.

24

27. Sawada T, Shite J, Garcia-Garcia HM, Shinke T, Watanabe S, Otake H, Matsumoto D, Tanino Y, Ogasawara D, Kawamori H, Kato H, Miyoshi N, Yokoyama M, Serruys PW, Hirata K. Feasibility of combined use of intravascular ultrasound radiofrequency data analysis and optical coherence tomography for detecting thin-cap fibroatheroma. Eur Heart J 2008;29:1136-46.

28. Nakano M, Otsuka F, Virmani R. Letter by Nakano et Al regarding article, "optical coherence tomographic analysis of in-stent neoatherosclerosis after drug-eluting stent implantation". Circulation 2011;124:e954.

Figure legends

Figure 1. An example of an attenuated plaque with a maximal arc of attenuation $\geq 30°$ A: Grayscale image obtained by 40MHz transducer showed attenuated plaque with maximal arc of attenuation of 93°. B: Grayscale image obtained by 20MHz transducer showed no definite attenuation. C: VH-TCFA at the maximal attenuation site. D–F: OCT images showed disrupted thin cap with plaque rupture (D, arrow) and microchannel (D, arrowhead) at the maximal attenuation site; OCT-TCFA (E, arrow) and macrophages (E, arrowheads) proximal segment to the maximal attenuation site; and cholesterol crystal (F).

Figure 2. An example of a plaque with a maximal arc of IVUS attenuation <30° A: Grayscale image obtained by 40MHz transducer showed a small IVUS attenuation with a maximal arc of attenuation of 21°. B: At the corresponding site, VH-defined plaque compositions were fibrous 55%, fibro-fatty 42%, and necrotic core 3%. C: OCT showed the thickness of fibrous cap >200 μm.

Figure 3. A: Relationship between the attenuation angles using 40MHz vs. 20MHz transducers at the maximal attenuation site.

Figure 4. A: ROC analysis determining the cut-off values of the maximal attenuation angle (using 40MHz transducer) to predict the presence of VH-TCFA. B: Comparison of predictabilities of the maximal arc of attenuation $\geq 30°$ using 40MHz vs. 20MHz transducers for the prediction of VH-TCFA.

Figure 5. A: ROC analysis determining the cut-off values of the maximal attenuation angle (using 40MHz transducer) to predict the presence of OCT-TCFA. B: ROC analysis determining the cut-off values of the maximal attenuation angle (using 40MHz transducer) to predict the presence of OCT-defined plaque rupture. C: Comparison of predictabilities of

25

the maximal arc of attenuation $\geq 30°$ using 40MHz vs. 20MHz transducers for the

prediction of OCT-TCFA.

Table 1. Clinical and angiographic and IVUS data in 115 patients with 115 lesions

Variable	Total	Lesions with attenuation ≥30° (40MHz)	Lesions with attenuation <30° (40MHz)	p value
N	115	71	44	
Clinical characteristics				
Age (years)	62.0 (56.0 – 69.0)	64.0 (57.0 – 71.0)	59.0 (55.0 – 66.0)	0.039
Male, N (%)	84 (73%)	61 (86%)	23 (52%)	<0.001
Smoking, N (%)	46 (40%)	33 (47%)	13 (30%)	0.072
Hypertension, N (%)	73 (64%)	44 (62%)	29 (66%)	0.670
Statin at admission, N (%)	75 (65%)	47 (66%)	28 (64%)	0.779
Diabetes mellitus, N (%)	28 (24%)	20 (28%)	8 (18%)	0.268
Acute coronary syndrome, N (%)	35 (30%)	26 (37%)	9 (21%)	0.050
Total cholesterol, mg/dl	159.0 (136.0 – 195.0)	160.0 (146.0 – 199.0)	154.5 (123.2 – 188.0)	0.070
HDL-cholesterol, mg/dl	43.0 (36.0 – 52.0)	42.0 (33.0 – 50.0)	46.0 (38.3 – 54.5)	0.026

1

LDL-cholesterol, mg/dl	93.6 (64.0 – 111.8)	94.6 (71.0 – 114.8)	85.8 (54.0 – 106.5)	0.027
Pre-PCI peak CK-MB (ng/ml)	1.0 (0.6–2.0)	1.1 (0.7–2.4)	0.9 (0.4–1.3)	0.020[#]
Grayscale IVUS data				
Proximal reference EEM area, mm^2	15.5 (11.8 – 20.0)	16.1 (12.4 – 22.0)	14.1 (11.7 – 16.4)	0.001
Distal reference EEM area, mm^2	10.2 (7.8 – 14.0)	10.2 (7.8 – 14.1)	9.9 (7.9 – 13.9)	0.649
MLA, mm^2	2.5 (1.6 – 3.7)	2.1 (1.4 – 3.1)	3.4 (2.0 – 4.1)	0.001
EEM area at the MLA site, mm^2	11.5 (8.7 – 14.8)	12.6 (9.6 – 15.3)	9.9 (7.2 – 13.4)	0.003
Plaque burden, %	78.1 (67.9 – 84.8)	80.7 (76.7 – 87.3)	66.9 (59.1 – 76.0)	<0.001
Remodeling index	0.91 (0.77 – 1.03)	0.95 (0.84 – 1.06)	0.83 (0.71 – 0.96)	0.008
Maximal attenuation angle by 20MHz	0 (0 – 45.0)	20 (0 – 100)	0 (0 – 0)	<0.001
Maximal attenuation angle $\geq$30° by 20MHz, N (%)	33 (29%)	33 (47%)	0 (%)	<0.001

Median (inter–quartile ranges), p values using non –parametric Mann-Whitney test

MLA: minimal lumen area, EEM: external elastic membrane

[#] nonparametric test (Mann-Whitney), Median (inter-quartile ranges)

2

Table 2. VH-IVUS findings

Variable	Total	Lesions with attenuation ≥30° (40MHz)	Lesions with attenuation <30° (40MHz)	p value
Lesion, N	115	71	44	
At the maximal necrotic core site				
fibrous, %	47.4 (35.9 – 57.7)	45.1 (35.4 – 52.2)	57.3 (38.9 – 64.9)	0.005
fibrofatty, %	3.6 (1.3 – 7.0)	3.3 (1.4 – 6.1)	4.2 (1.0 – 11.3)	0.116
necrotic core, %	35.7 (29.0 – 44.0)	38.1 (33.1 – 44.7)	27.9 (18.7 – 39.1)	<0.001
dense calcium, %	10.2 (3.9 – 19.1)	12.0 (5.9 – 20.1)	5.4 (1.8 – 18.3)	0.017
VH-TCFA, N (%)	71 (62%)	54 (76%)	17 (39%)	<0.001
Presence of VH-TCFA, N (%)	80 (69%)	59 (83%)	21 (47%)	<0.001
VH-TCFA at the MLA site	36 (31%)	23 (32%)	13 (30%)	0.749
VH-TCFA proximal to the MLA	46 (40%)	35 (49%)	11 (25%)	0.010
VH-TCFA distal to the MLA	22 (19%)	12 (17%)	10 (23%)	0.440

* assessed by 40MH IVUS

Median (inter-quartile ranges), p values using non –parametric Mann-Whitney test

1

Table 3. OCT findings

Variable	Total	Lesions with attenuation ≥30° (40MHz)	Lesions with attenuation <30° (40MHz)	p value
Lesion, N	115	71	44	
OCT-MLA, mm^2	2.0 (1.4 – 3.2)	2.0 (1.1 – 2.6)	2.5 (1.5 – 4.1)	0.019
Presence of lipid, N (%)	105 (91%)	71 (100%)	34 (77%)	<0.001
Maximal angle of lipid, °	200.0 (90.0 – 280.0)	250.0 (180.0 – 200.0)	85.0 (30.0 – 150.0)	<0.001
Calcification, N (%)	72 (63%)	48 (68%)	24 (55%)	0.159
Thickness of fibrous cap, μm	70.0 (60.0 – 120.0)	60.0 (50.0 – 80.0)	120.0 (82.5 – 150.0)	<0.001
Macrophage, N (%)	57 (50%)	50 (70%)	7 (16%)	<0.001
Cholesterol crystal, N (%)	22 (19%)	18 (25%)	4 (9%)	0.031
Microchannels, N (%)	73 (64%)	54 (76%)	19 (43%)	<0.001
Presence of OCT-TCFA, N (%)	57 (50%)	50 (70%)	7 (16%)	<0.001
OCT-TCFA at the MLA site	34 (30%)	30 (42%)	4 (9%)	<0.001
OCT-TCFA proximal to the MLA	39 (34%)	36 (51%)	3 (7%)	<0.001

1

OCT-TCFA distal to the MLA	19 (17%)	17 (24%)	2 (5%)	0.006
Plaque rupture, N (%)	41 (36%)	37 (52%)	4 (9%)	<0.001
Rupture at the MLA site	29 (25%)	26 (37%)	3 (7%)	<0.001
Rupture proximal to the MLA	18 (16%)	18 (25%)	0 (0%)	<0.001
Rupture distal to the MLA	9 (8%)	8 (11%)	1 (2%)	0.081
Presence of thrombi, N (%)	41 (36%)	36 (51%)	5 (11%)	<0.001
Red thrombi, N (%)	15 (13%)	13 (18%)	2 (5%)	<0.001
White thrombi, N (%)	40 (35%)	35 (49%)	5 (11%)	<0.001

Median (inter-quartile ranges), p values using non –parametric Mann-Whitney test

2

* assessed by 40MH IVUS

3

Table 4. Tissue characteristics of the maximal attenuation site in 71 lesions

| Variable	Lesions with maximal attenuation ≥30° (40MHz)
OCT findings at the maximal attenuation site	
Lipidic plaque, N (%)	71 (100%)
Calcification, N (%)	27 (38%)
OCT-TCFA, N (%)	37 (52%)
Plaque rupture, N (%)	32 (45%)
Macrophage, N (%)	43 (61%)
Cholesterol crystal, N (%)	16 (23%)
Thrombi, N (%)	31 (43%)
VH-IVUS findings at the maximal attenuation site	
fibrous, %	56.1 (44.4 – 63.9)
fibrofatty, %	18.0 (9.3 – 23.3)
necrotic core, %	19.7 (11.6 – 27.8)
dense calcium, %	5.6 (1.2 – 10.7)
Fibroatheroma,%	65 (94%)
VH-TCFA, (%)	33 (47%)
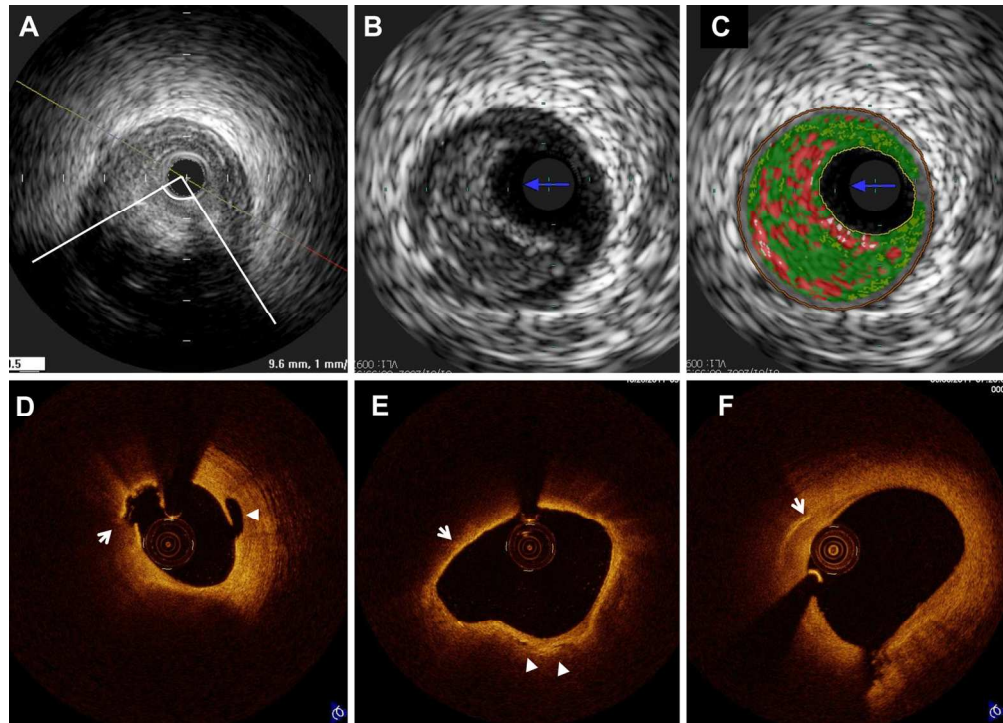
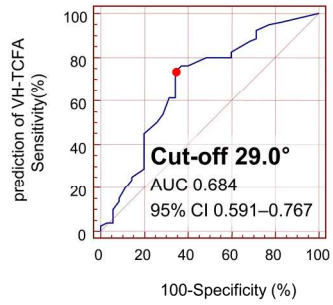attenuated plaque with a maximal arc of attenuation ≥30°
175x125mm (300 x 300 DPI)
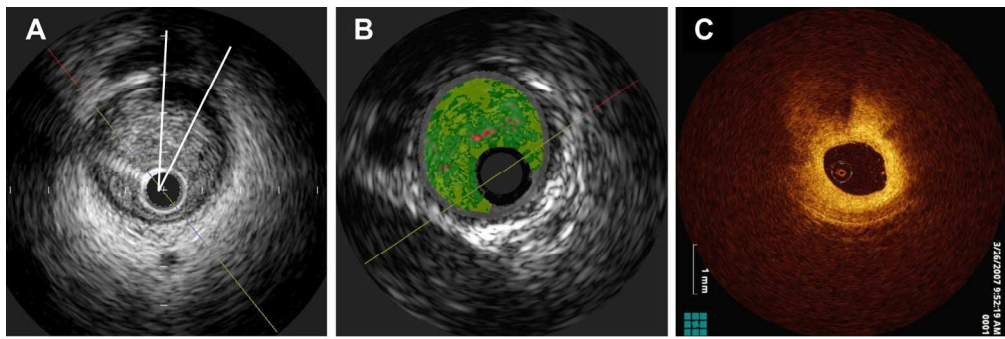
maximal arc of IVUS attenuation <30°
175x57mm (300 x 300 DPI)

40MHz vs. 20MHz
95x73mm (600 x 600 DPI)

A

Cut-off 29.0°
AUC 0.684
95% CI 0.591–0.767
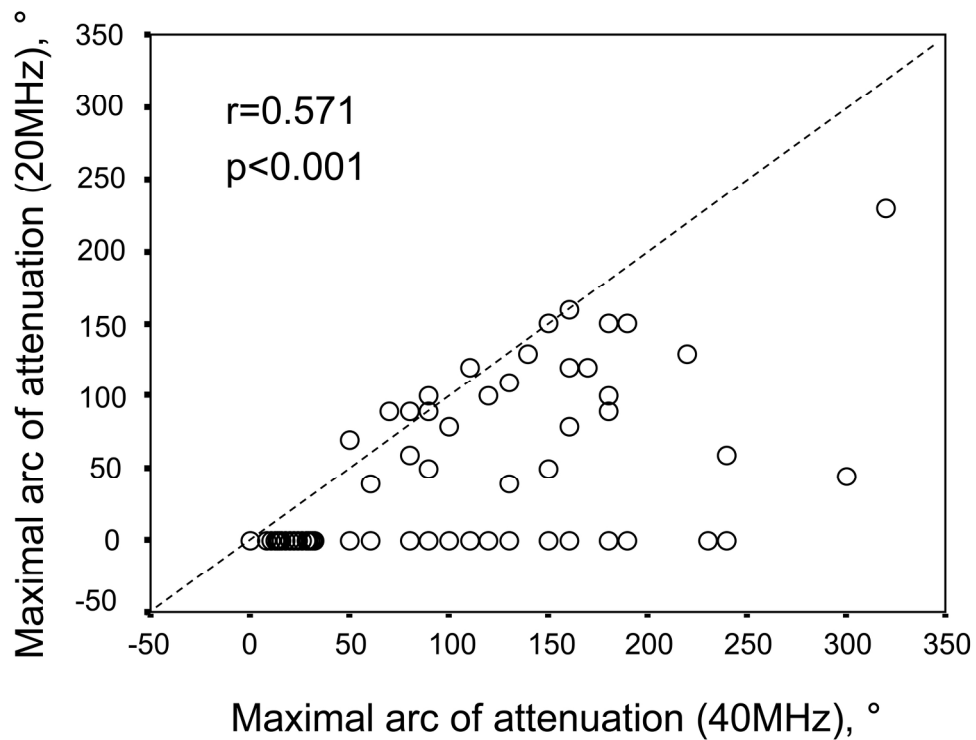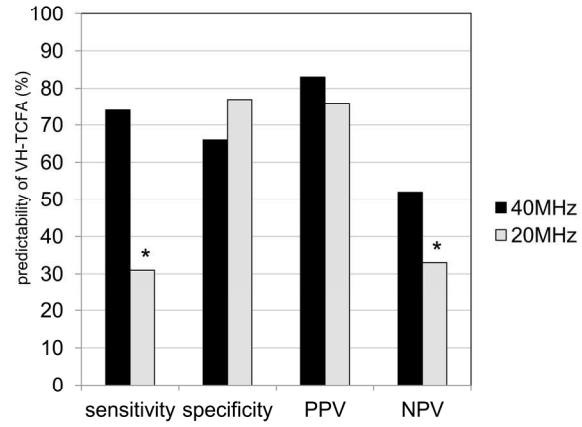
Sensitivity 74%
Specificity 66%
PPV 83%
NPV 52%

B

*p value <0.05 vs. 40MHz

ROC analysis
99x56mm (600 x 600 DPI)

A

Sensitivity 89%
Specificity 64%
PPV 70%
NPV 84%

B

Sensitivity 83%
Specificity 64%
PPV 57%
NPV 87%

C

*p value <0.05 vs. 40MHz
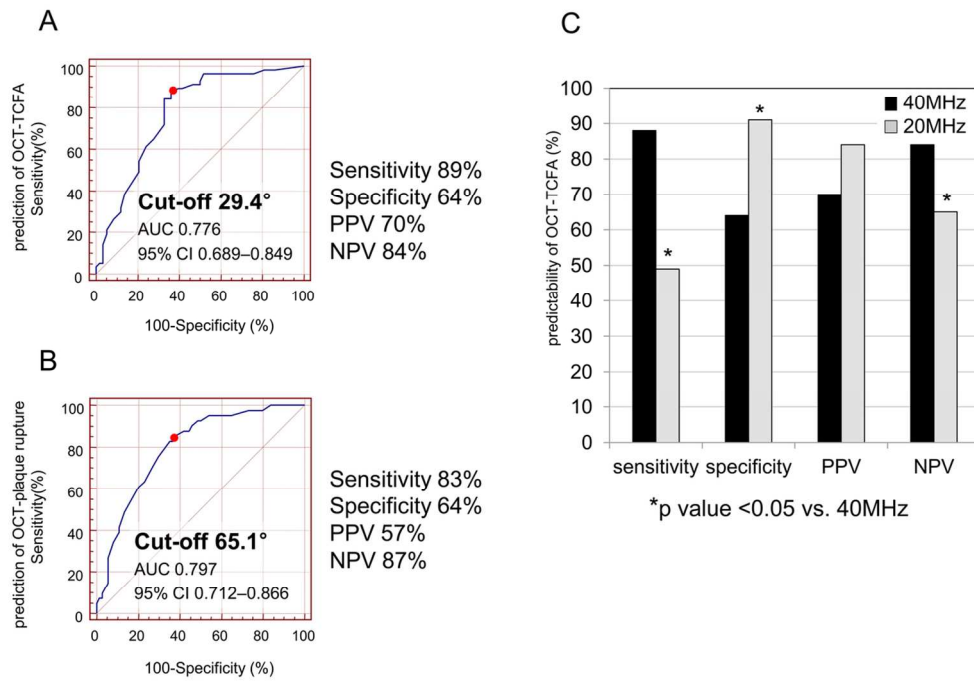
OCT-TCFA
119x81mm (300 x 300 DPI)